J Mol Model (2007) 13:993–1000
DOI 10.1007/s00894-007-0221-8

ORIGINAL PAPER

3D-QSAR studies on fluoropyrrolidine amides as dipeptidyl peptidase IV inhibitors by CoMFA and CoMSIA

Juan Zeng · Guixia Liu · Yun Tang · Hualiang Jiang

Received: 21 November 2006 / Accepted: 23 May 2007 / Published online: 6 July 2007

Abstract Three-dimensional quantitative structure-activity relationship (3D-QSAR) analyses using CoMFA and CoMSIA methods were conducted on a series of fluoropyrrolidine amides as dipeptidyl peptidase IV (DP-IV) inhibitors. The selected ligands were docked into the binding site of the 3D model of DP-IV using the GOLD software, and the possible interaction models between DP-IV and the inhibitors were obtained. Based on the binding conformations of these fluoropyrrolidine amides and their alignment inside the binding pocket of DP-IV, predictive 3D-QSAR models were established by CoMFA and CoMSIA analyses, which had conventional r^2 and cross-validated coefficient values (r^2_{cv}) up to 0.982 and 0.555 for CoMFA and 0.953 and 0.613 for CoMSIA, respectively. The predictive ability of these models was validated by six compounds that were in the testing set. Structure-based investigations and the final 3D-QSAR results provide the guide for designing new potent inhibitors.

Keywords CoMFA · CoMSIA · Diabetes mellitus · Dipeptidyl peptidase IV (DP-IV) · 3D-QSAR

J. Zeng · G. Liu (✉) · Y. Tang · H. Jiang
Laboratory of Molecular Modeling & Design,
School of Pharmacy,
East China University of Science and Technology,
Shanghai 200237, People's Republic of China
e-mail: gxliu@ecust.edu.cn

H. Jiang
Shanghai Institute of Materia Medica,
Chinese Academy of Sciences,
Shanghai 201203, People's Republic of China

Introduction

Type 2 diabetes, also known as non-insulin-dependent diabetes mellitus (NIDDM) or adult onset diabetes, accounts for 90–95% of the cases of diabetes. People with type 2 diabetes usually develop the condition after age 45, and the risk for getting it increases with age. However, the number of children with type 2 diabetes is increasing rapidly. The high prevalence of diabetes is combined with the associated increased mortality and morbidity, primarily as a result of macrovascular disease and microvascular long-term complications [1, 2]. Thus, there is an imperative need for potent therapeutic approaches for glycemic control.

Dipeptidyl peptidase IV (DP-IV, also known as CD 26) which is a glycoprotein, consists of 766 amino acids in humans and 767 amino acids in rats [3]. DP-IV is a membrane-associated serine protease which is widely distributed in mammalian tissues and body fluids [4]. It modulates the biological activity of several peptide hormones, chemokines and neuropeptides by specifically cleaving X-proline or X-alanine dipeptides from the N-terminus [5]. Glucagon-like peptide-1 (GLP-1), which is expressed not only in pancreatic α-cells but also in the L-cells of the intestinal mucosa [6, 7], is secreted in response to the absorption of glucose, other sugars, fatty acids and to a minor extent amino acids [8, 9]. It plays an important role in the regulation of postprandial insulin release. However, DP-IV rapidly cleaves the active form of GLP-1 (GLP-1[7–36] amide) to its inactive form (GLP-1[9–36] amide) with a half-life of approximately one minute, and is thought to be the primary enzyme responsible for this hydrolysis [10]. Those animals having defective DP-IV activity or gene deletion of DP-IV are resistant to develop glucose intolerance on feeding of a high-

fat diet [3, 11]. Therefore, inhibition of DP-IV is a novel therapeutic approach for the treatment of type 2 diabetes.

During the past few years, a large number of compounds were synthesized and evaluated as DP-IV inhibitors. Among them, cyanopyrrolidine derivatives were proved to be potent. However, they were irreversible inhibitors [12–14]. Recently much attention has been paid to the reversible inhibitors [15–20]. Based on the structures available, Caldwell and co-workers [21] designed and synthesized a series of fluoropyrrolidine amides as reversible inhibitors of DP-IV, and their inhibitory activities were also measured (Tables 1 and 2).

In the present study, we investigated the binding mode of these fluoropyrrolidine amides with DP-IV using molecular docking approach. Following the docking results, 3D-QSAR models were constructed by using comparative molecular field analysis (CoMFA) and comparative molecular similarity analysis (CoMSIA). The purpose of this study is to offer some beneficial clues in structural modifications for designing new inhibitors with much higher inhibitory activities against DP-IV, and a predictive model for evaluating novel synthetic candidates. The first CoMFA study on DP-IV inhibitors was done in 1993 when the X-ray structure of DP-IV was not available [22]. It successfully demonstrated that QSAR was a useful tool for obtaining more effective inhibitor structures.

Computational details

Biological data and molecular structures

Tables 1 and 2 show a series of DP-IV amides inhibitors synthesized by Caldwell et al. in 2004 [21], which were divided into a training set and a testing set. The training set consisted of 27 compounds, and the testing set, which was selected randomly, comprised 6 compounds. The compounds in the training set were employed to build 3D-QSAR models, and those in the testing set were used to evaluate the 3D-QSAR models. The IC_{50} values of the inhibitors were converted into pIC_{50} ($-logIC_{50}$) and used as dependent variables in the CoMFA and CoMSIA calculations.

The 3D structures of all compounds were constructed by using molecular modeling software package Sybyl version 7.0 [23] and energetically minimized using the Tripos force field [24] with Gasteiger-Hückel charges [25]. The crystal

Table 1 Structures and in vitro DP-IV inhibitory activity of cyclohexylglycine amides

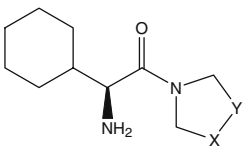

Compd	X – Y	DP-IV IC_{50}(nM)	$-logIC_{50}$
DP15	CF_2-CH_2	73	7.14
DP20	S-CH_2	89	7.05
DP23*	CHF-CH_2(S)-	170	6.77
DP29	CH_2-CH_2	320	6.49
DP30	CHF-CH_2(R)-	340	6.47

Table 2 Structures and in vitro DP-IV inhibitory activity of 4-aminocyclohexylglycine derivatives

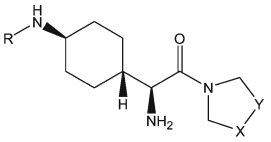

Compd	R	X - Y	DP-IV IC_{50}(nM)	$-logIC_{50}$
DP01	SO_2(2,4-$F_2C_6H_3$)	CF_2-CH_2	21	7.68
DP02	SO_2(4-(CF_3O)C_6H_4)	S-CH_2	22	7.66
DP03	SO_2(4-(CF_3O)C_6H_4)	CF_2-CH_2	23	7.64
DP04	Cbz	S-CH_2	25	7.60
DP05	Cbz	CF_2-CH_2	27	7.57
DP06	SO_2(4-(CF_3O)C_6H_4)	CHF-CH_2(S)-	35	7.46
DP07	SO_2(2,4-$F_2C_6H_3$)	CHF-CH_2(S)-	48	7.32
DP08	CO(3,4-$F_2C_6H_3$)	S-CH_2	53	7.28
DP09	CO(3,4-$F_2C_6H_3$)	CHF-CH_2(S)-	54	7.27
DP10	CO(3,4-$F_2C_6H_3$)	CF_2-CH_2	55	7.26
DP11	Cbz	CHF-CH_2(S)-	56	7.25
DP12*	SO_2(2,4-$F_2C_6H_3$)	CHF-CH_2(R)-	58	7.24
DP13	CO(2-(CF_3)C_6H_4)	S-CH_2	67	7.17
DP14*	CO(2-(CF_3)C_6H_4)	CF_2-CH_2	70	7.15
DP16	SO_2(4-(CF_3O)C_6H_4)	CHF-CH_2(R)-	75	7.12
DP17*	Cbz	CHF-CH_2(R)-	88	7.06
DP18	SO_2(2,4-$F_2C_6H_3$)	CH_2-CH_2	88	7.06
DP19	SO_2(4-(CF_3O)C_6H_4)	CH_2-CH_2	89	7.05
DP21	Cbz	CH_2-CH_2	94	7.03
DP22	CO(3,4-$F_2C_6H_3$)	CHF-CH_2(R)-	110	6.96
DP24*	CO(3,4-$F_2C_6H_3$)	CH_2-CH_2	190	6.72
DP25	CO(2-(CF_3)C_6H_4)	CHF-CH_2(S)-	210	6.68
DP26	CO(2-(CF_3)C_6H_4)	CHF-CH_2(R)-	250	6.60
DP27	SO_2(2,4-$F_2C_6H_3$)	CHF-CHF(R,R)-	250	6.60
DP28	SO_2(4-(CF_3O)C_6H_4)	CHF-CHF(R,R)-	270	6.57
DP31	Cbz	CHF-CHF(R,R)-	360	6.44
DP32	Cbz	CHF-CHF(S,S)-	830	6.08
DP33*	SO_2(4-(CF_3O)C_6H_4)	CHF-CHF(S,S)-	870	6.06

* Compounds those were not included in the construction of 3D-QSAR models

structure of DP-IV in complex with its inhibitor Val-Pyr (PDB entry code 1N1M) was recovered from Brookhaven Protein Database (PDB, http://www.pdb.org/pdb/home/home.do). After adding all the hydrogen atoms, the Val-Pyr/DP-IV complex was relaxed 300 steps using Tripos force field [24] with Kollman all-atom charges [26] for enzyme and Gasteiger-Hückel charges [25] for ligand in Sybyl. All calculations were performed on a Dell Precision 670 workstation running Redhat Linux WS 3.0.

Molecular docking

To locate the appropriate binding orientations and conformations of these fluoropyrrolidine amide inhibitors interacting with DP-IV, the advanced molecular docking program GOLD version 3.0 [27] was employed to dock the inhibitors into the active site of DP-IV. GOLD uses a powerful genetic algorithm (GA) method for conformational search, and has been evaluated as one of the best docking programs. The active site was defined as protein residues within 10 Å around the cocrystallized ligand. The scoring functions used to score and rank the dockings was ChemScore [28] fitness function. The settings for the genetic algorithm runs were kept at their default values. The maximum number of GA runs was set to 10 for each compound. Those docked conformations were saved in MOL2 format and then imported into Sybyl for further analysis.

3D-QSAR analyses

Based on the conformational alignments derived from the molecular docking, the CoMFA [29] and CoMSIA [30] studies were performed on these inhibitors to analyze the specific contributions of steric, electrostatic, hydrophobic, and hydrogen bond effects on bioactivities of the inhibitors.

CoMFA studies

The overlapped molecules were placed in a 3D lattice with regular grid points separated by 2 Å. The van der Waals potential and Coulombic term representing the steric and electrostatic fields were calculated using standard Tripos force field for CoMFA. An sp^3 carbon atom with a formal charge of +1 served as the probe atom to generate steric (Lennard-Jones 6–12 potential) and electrostatic (Coulombic potential) field energies. A distance-dependent dielectric constant was used. The steric and electrostatic fields were truncated at ±30.00 kcal mol^{-1}. With standard options for scaling of variables, the regression analysis was carried out using the full cross-validated partial least squares (PLS) method (leave-one-out). The minimum-sigma (column filtering) was set to 2.0 kcal mol^{-1} to improve the signal-to-noise ratio by omitting those lattice points whose energy variation was below this threshold. The final model, noncross-validated conventional analysis, was developed with the optimum number of components equal to that yielding the highest q^2.

CoMSIA studies

In this study, five physicochemical properties, namely steric, electrostatic, hydrophobic, hydrogen bond donor and acceptor, were evaluated. These fields were selected to cover the major contributions to ligand binding. For a molecule j with atoms i at the grid point q, the CoMSIA similarity indices $A_{F,k}$ were calculated by the equation as follows:

$$A^q_{F,k}(j) = -\sum_{i=1}^{n} W_{\text{probe},k} W_{ik} e^{-\alpha r^2_{iq}},$$

where A is the similarity index at grid point q, summed over all atoms i of the molecule j under investigation; $W_{\text{probe},k}$ is the probe atom with radius 1 Å, charge +1, hydrophobicity +1, hydrogen bond donating +1, hydrogen bond accepting +1; W_{ik} is the actual value of the physicochemical property k of atom i; r_{iq} is the mutual distance between the probe atom at grid point q and atom i of the test molecule; α is the attenuation factor, and the default value of a is 0.3 [31]. The statistical evaluation for the CoMSIA analyses was performed in the same way as described for CoMFA.

Results and discussion

Interactions between inhibitors and DP-IV

Inhibitor's conformation

Ten conformations were obtained through GOLD for each ligand; and the conformation with the strongest predicted binding affinity to DP-IV was selected as the possible binding conformation. The conformational superposition of Val-Pyr from the X-ray crystal structure and that from the GOLD result was shown in Fig. 1. The root-mean-square deviation (RMSD) between these two conformations was equal to 0.611 Å, denoting a high docking reliability of GOLD in reproducing the experimentally observed binding mode for DP-IV inhibitors. The small RMSD value also indicated that the parameter set for the GOLD simulation was reasonable to reproduce the X-ray structure. Therefore, the GOLD method and the parameter set could be extended to search the binding conformations of other inhibitors. Thus, the most possible binding conformations of 27 compounds in the training set and 6 compounds in the testing set were obtained. The alignment of the docking

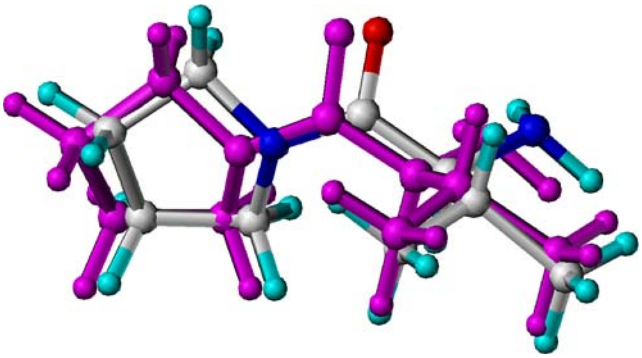

Fig. 1 Conformational comparison of Val-Pyr from the crystal structure (magenta) and that from the GOLD result (by atom type color)

conformation of all 33 compounds was shown in Fig. 2. As shown in Fig. 2, just like Val-Pyr cocrystallized with DP-IV, fluoropyrrolidine amides located in the region of the inside cavity in similar conformations, indicating they share some common binding features.

Binding mode of inhibitors

To elucidate the interaction mechanism, compound DP01, the most potent inhibitor among the 33 compounds, was selected for more detailed analysis. The interacting model of inhibitor DP01 with DP-IV was generally depicted in Fig. 3. The pyrollidine ring moieties of the ligands almost located at the same site, which were buried in a hydrophobic pocket formed by the side chains of Tyr547, Tyr631, Val656, Tyr662, Tyr666, and Val711. Tyr662 and Tyr666 respectively stacked at each side of the pyrollidine rings of the inhibitors, with Tyr662 in a parallel fashion and Tyr666 in an orthogonal fashion. In addition, the X substituent of DP01 appeared to have polar interactions with vicinal residues, such as Tyr631, Tyr662, and Tyr666. The carbonyl group, which linked the pyrollidine, formed a hydrogen bond to the side chain of Asn710. Two glutamic acids, Glu205 and Glu206, formed strong hydrogen bonds to the amino group of inhibitors, which corresponded to the N terminus of a peptide substrate [32]. The cyclohexyl moieties pointing to the large cavity had hydrophobic contacts with hydrophobic residues Phe357 and Tyr666. The R substituents, which might be exposed to the solvent, located at different positions, whereas other moieties situated much at the same site. In our models, when the R group was replaced by SO_2(4-(CF_3O)C_6H_4) or SO_2(2,4-$F_2C_6H_3$), the NH group which linked the cyclohexyl to the R substituent, could interact with the OH group of the side chain of Tyr547 by forming a hydrogen bond. Meanwhile, the benzene ring formed a π-π stacking interaction with Tyr547.

3D-QSAR models

3D-QSAR models of fluoropyrrolidine amide compounds were generated based on the binding conformations and their alignment of 27 molecules (Tables 1 and 2) in the active site of DP-IV. A testing set of six molecules (Tables 1 and 2, star labeled) was used to test the external prediction of the model. The best predictions were obtained with the CoMFA standard model (q^2=0.555, r^2=0.982) and CoM-

Fig. 2 Alingment of compounds

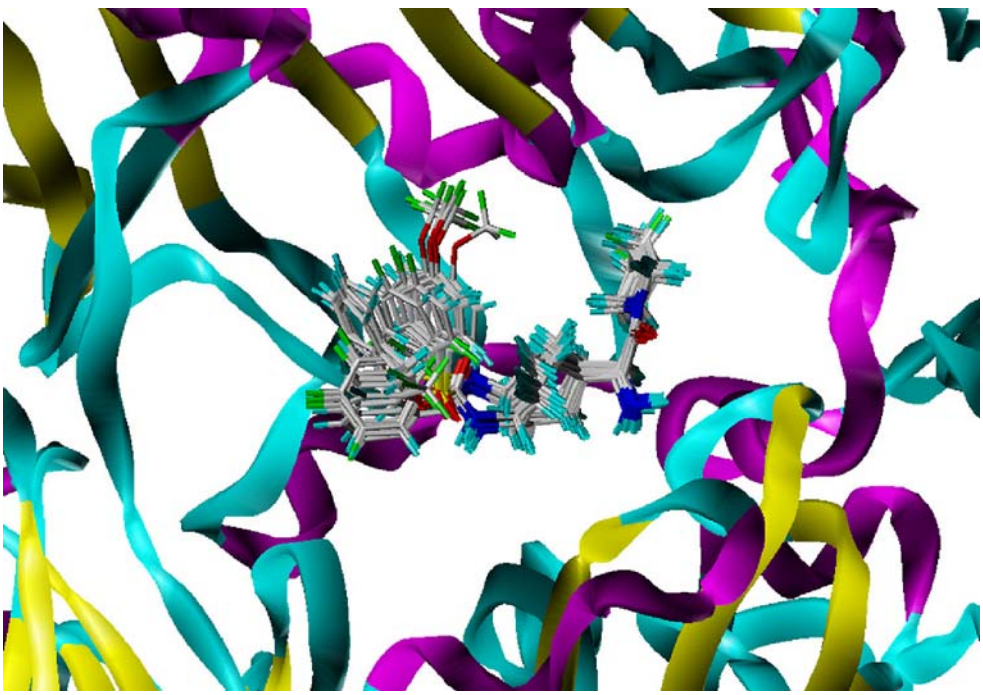

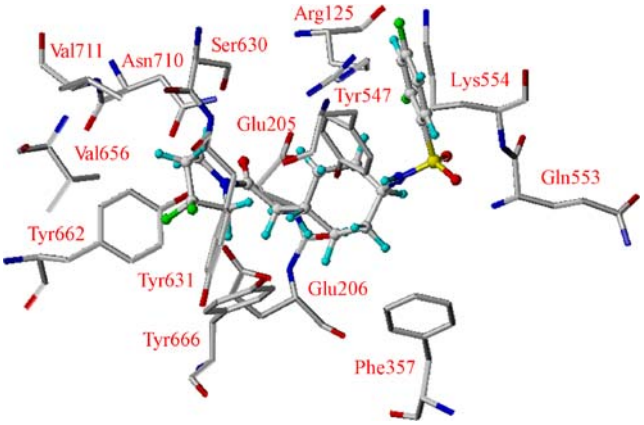

Fig. 3 Proposed interaction model of inhibitor DP01 in the active site of DP-IV. The inhibitor and the residues of active site are represented by ball-and-stick and stick models, respectively

SIA combined steric, electrostatic, hydrophobic, and hydrogen bond donor/acceptor fields (q^2=0.613, r^2=0.953). The results of CoMFA and CoMSIA were listed in Table 3. The predicted activities of the 33 inhibitors from the 3D-QSAR model versus their experimental activities were compiled in Tables 4 and 5, and the correlations between predicted activity and experimental activity were presented in Fig. 4, which indicated a good conventional statistical correlation.

Six inhibitors (DP12, DP14, DP17, DP23, DP24, and DP33 in Tables 1 and 2) that were not included in the training set were randomly selected as testing compounds to validate the QSAR models. The predicted -logIC_{50} values of the six testing compounds were in good agreement with the experimental data in a statistically tolerable error range (Table 5), with a correlation coefficient of $r^2_{pred} = 0.884$ and 0.914 for CoMFA and CoMSIA models, respectively, indicating that the CoMFA and CoMSIA models which were based on 27 inhibitors were reliable and had a good ability of prediction. From these results, we conclude that the constructed CoMFA and CoMSIA models are reliable and could be used for designing new inhibitors against DP-IV.

CoMFA contour maps

The CoMFA steric and electrostatic fields based on the alignment of the binding conformations were shown as contour plot in Fig. 5a. The most potent compound DP01 was displayed in the map in aid of visualization. The CoMFA steric contours indicate the areas where steric bulky substituents may have favorable (green) or unfavorable (yellow) effects on the inhibitory activity of an inhibitor. The electrostatic contours suggest that increasing the negative charge into areas contoured in red will enhance the binding affinity, whereas groups of the ligands with a more positive charge will improve the binding affinity in areas colored in blue.

The steric contour of CoMFA (Fig. 5b) showed a large green contour around the phenyl group of the template structure. This indicated that bulky substituents in this region would increase the DP-IV inhibitory activity. When other moieties were identical except the R substituents, those compounds possesing sulfonyl groups had good inhibitory potency, with an exception of compound DP33. This may be due to the orientation of their phenyl groups toward sterically favored green contour, and thus the benzene ring formed favorable interaction with Tyr547. The steric contours showed yellow contour near sulfonyl group of DP01. At this position bulky substituents were not tolerated, and therefore the molecules with CO(3,4-$F_2C_6H_3$) or CO(2-$(CF_3)C_6H_4$) showed low activity. The benzene rings of their R substituents located near the yellow contour, and probably had unfavorable steric collisions with environmental residue Gln553.

There was a large blue contour close to the Y substituent of the pyrollidine ring of DP01. This contour could be used to explain why those molecules substituted by a fluorine atom in the Y substituent were much less potent such as DP27, DP28, DP31, DP32, and DP33. This positive-charge-favored region was observed near the residues of Ser630 and Asn710, which implied that electron deficient groups might interact with the side chains of these residues and therefore increased the inhibitory potencies. A red contour

Table 3 Statistical indexes of CoMFA and CoMSIA models based on 27 fluoropyrrolidine amides binding conformers

	Cross-validated		Conventional		
	$q^2(r_{cross}{}^2)$	Optimal comp.	r^2	S	F
CoMFA	0.555	6	0.982	0.066	184.286
CoMSIA	0.613	5	0.953	0.104	85.359
Field Distribution (%)					
	Steric	Electrostatic	Hydrophobic	H-bond donor	H-bond receptor
CoMFA	43.6	56.4			
CoMSIA	7.9	36.9	25.2	11.7	18.4

Table 4 Predicted activities vs experimental activities (-logIC_{50}) and residues (δ) by CoMFA and CoMSIA of the training set

Compd	Experimental activity	CoMFA		CoMSIA	
		Predicted activity	δ	Predicted activity	δ
DP01	7.68	7.70	−0.02	7.73	−0.05
DP02	7.66	7.62	0.04	7.76	−0.10
DP03	7.64	7.66	−0.02	7.60	0.04
DP04	7.60	7.62	−0.02	7.66	−0.06
DP05	7.57	7.61	−0.04	7.52	0.05
DP06	7.46	7.44	0.02	7.36	0.10
DP07	7.32	7.32	0.00	7.23	0.09
DP08	7.28	7.34	−0.06	7.33	−0.05
DP09	7.27	7.25	0.02	7.13	0.14
DP10	7.26	7.25	0.01	7.36	−0.10
DP11	7.25	7.25	0.00	7.28	−0.03
DP13	7.17	7.16	0.01	7.14	0.03
DP15	7.14	7.20	−0.06	7.20	−0.06
DP16	7.12	7.12	0.00	7.04	0.08
DP18	7.06	7.04	0.02	6.96	0.10
DP19	7.05	7.00	0.05	7.05	0.00
DP20	7.05	6.94	0.11	7.08	−0.03
DP21	7.03	6.95	0.08	7.00	0.03
DP22	6.96	6.94	0.02	6.85	0.11
DP25	6.68	6.69	−0.01	6.67	0.01
DP26	6.60	6.60	0.00	6.50	0.10
DP27	6.60	6.58	0.02	6.69	−0.09
DP28	6.57	6.70	−0.13	6.68	−0.11
DP29	6.49	6.61	−0.12	6.56	−0.07
DP30	6.47	6.40	0.07	6.42	0.05
DP31	6.44	6.37	0.07	6.34	0.10
DP32	6.08	6.16	−0.08	6.35	−0.27

near the X substituent of pyrollidine ring indicated that the substitution of hydrogen atom by a more negative group like a fluorine atom would increase the activity. It was observed that the molecules with a fluorine atom in X substituent were more active than those with a hydrogen atom.

Table 5 Predicted activities vs experimental activities (-logIC_{50}) and residues (δ) by CoMFA and CoMSIA of the testing set

Compd	Experimental activity	CoMFA		CoMSIA	
		Predicted activity	δ	Predicted activity	δ
DP12	7.24	7.23	0.01	7.21	0.03
DP14	7.15	7.11	0.04	7.16	−0.01
DP17	7.06	7.05	0.01	7.07	−0.01
DP23	6.77	6.70	0.07	6.71	0.06
DP24	6.72	6.79	−0.07	6.79	−0.07
DP33	6.06	6.52	−0.46	6.48	−0.42

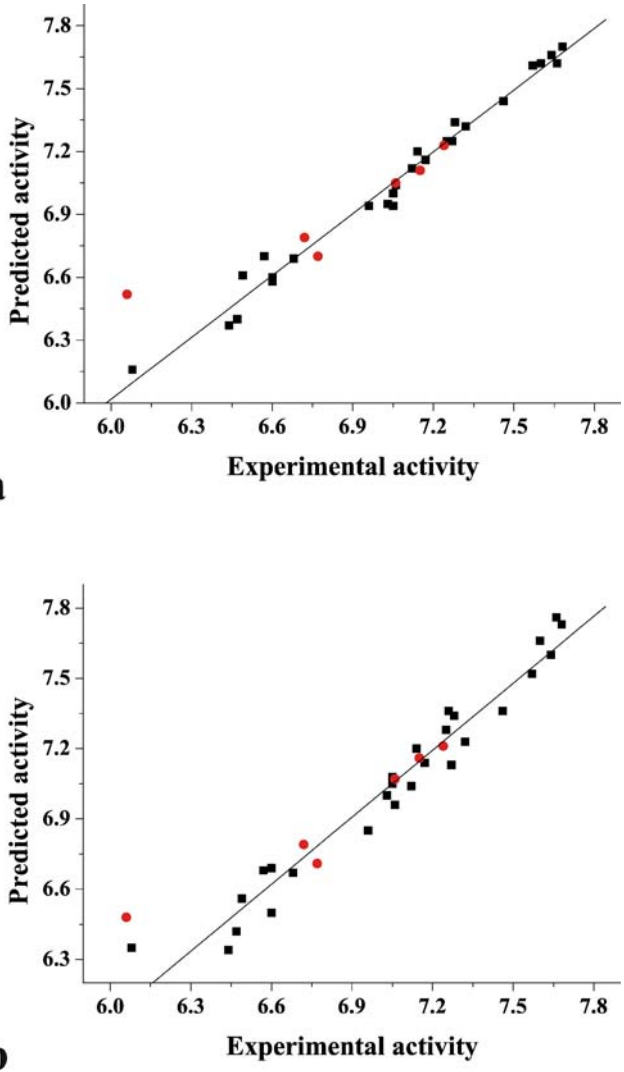

Fig. 4 Correlation between predicted activities by CoMFA (**a**) and CoMSIA (**b**) models and the experimental activities of training and testing sets. ▪, compounds of the training set; •, compounds of the testing set

CoMSIA contour maps

The CoMSIA contours were also displayed in Fig. 5. The steric and electrostatic field distributions of CoMSIA, as shown in Fig. 5b, were generally in accordance with the field distributions of CoMFA map.

The hydrophobic analysis of CoMSIA was depicted in Fig. 5c, where yellow and white colored regions represented hydrophobic and hydrophilic favorable areas, respectively. The region around X substituent of DP01 was surrounded by a yellow contour, suggesting hydrophobic substituents in this area could be beneficial to inhibitory activity against DP-IV. The introduction of fluorine atoms in the X substituent could improve the hydrophobicity of pyrrolidine ring. Accordingly, the compounds with two fluorine atoms in X substituent were more potent than that with one or no fluorine atom, for

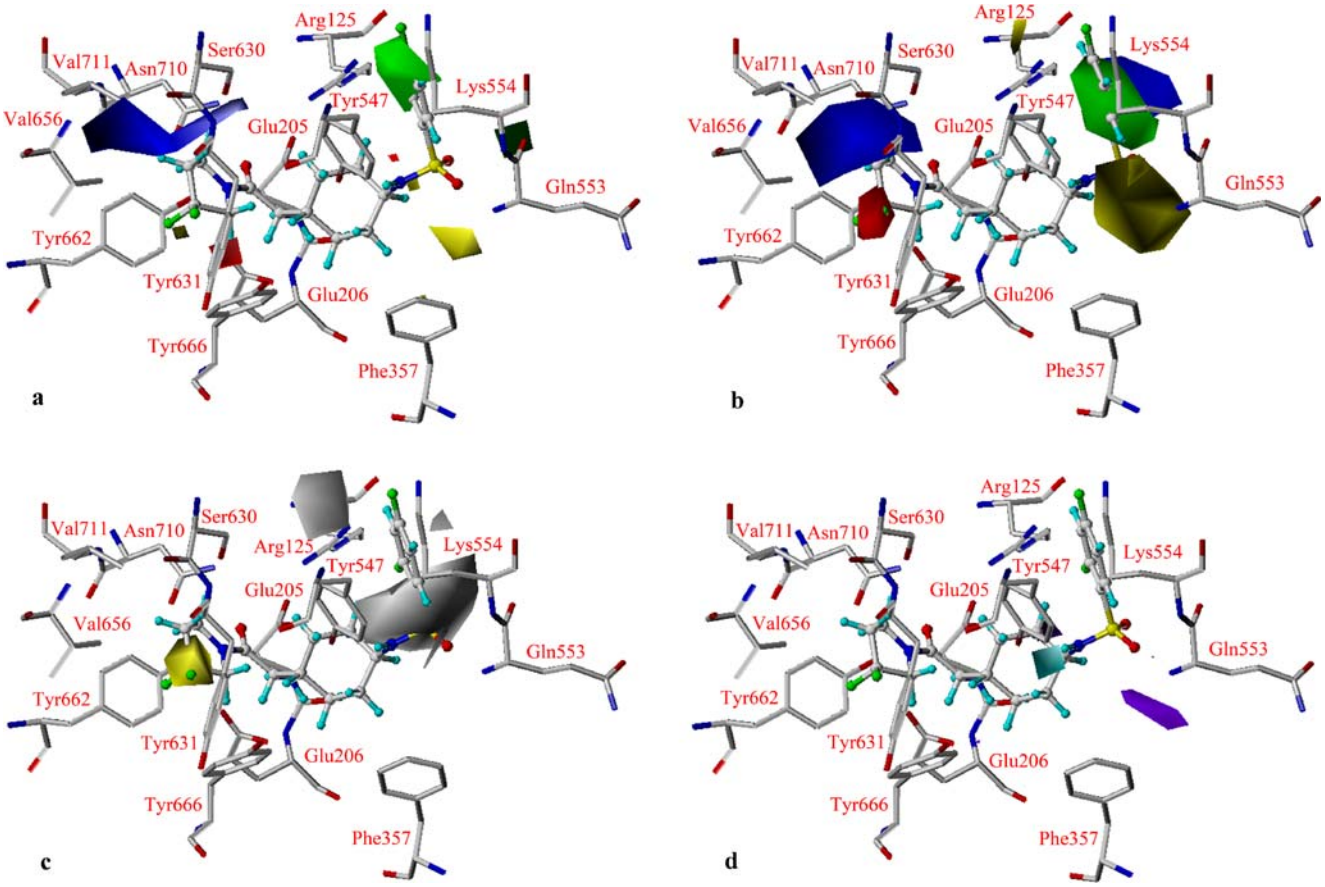

Fig. 5 Contour maps as compared with the topology of DP01-DP-IV complex. **a**) CoMFA; **b**) the steric and electrostatic field distributions of CoMSIA; **c**) the hydrophobic field distribution of CoMSIA; **d**) the H-bond donor and acceptor field distributions of CoMSIA. The residues are represented as sticks, and the inhibitor is shown in ball-and-stick. Sterically favored areas are in green; sterically unfavored areas are in yellow. Positive-charge-favored areas are in blue; positive-charge-unfavored areas are in red. Hydrophobic favored areas are in yellow; hydrophilic favored areas are in white. H-bond-donor-favored areas are in cyan; H-bond-donor-unfavored areas are in purple

example DP03>DP06(DP16)>DP19. On the other hand, the white contour embedded in the sulfonyl group moiety of DP01 suggested that more hydrophilic group substitutions in this place would increase inhibitory potency on account of the hydrophilicity of the environmental residues Gln553 and Lys554. Another white contour was seen in the vicinity of Ser630, which implied that more hydrophilic groups in this region might help to enhance inhibitory activity by interactions with hydrophilic residues Arg125 and Ser630. This could in part explain why compounds with SO_2(4-(CF_3O)C_6H_4) were slightly less active than those with SO_2(2,4-$F_2C_6H_3$).

The graphical interpretation of the field contributions of the hydrogen bond donor and acceptor was shown in Fig. 5d. Cyan contours indicate regions where hydrogen bond donor substituents on ligands are favorable, whereas purple contours represent areas where hydrogen bond donor properties on ligands are unfavorable. There was only one cyan contour in the hydrogen bond donor maps. It was adjacent to the NH that linked the cyclohexyl group of the R substituent. When the R group was substituted by SO_2(4-(CF_3O)C_6H_4) or SO_2(2,4-$F_2C_6H_3$), the NH group of the ligand could form a hydrogen bond with the side chain of Tyr547. This was one of the reasons why sulfonyl compounds relatively had potent activity.

Implication for new inhibitor design

The contour maps from both models are similar in explaining influence of substitution on activity. The substitution by di-fluorine on the 3-position of pyrrolidine ring may play an important role in binding to the DP-IV active site through hydrophobic interactions. Compounds with bulky substituents on aryl sulfonyl ring may increase the activity. For example, sterically naphthyl ring systems in place of phenyl ring of arylsulfonyl group can be tried for this purpose. Furthermore, the introduction of hydroxyl or amino group on the 6- or 7- position of naphthyl ring may show favorable effect on the inhibitory activity because a new hydrogen bond could be formed between the inhibitor and Lys554. The information obtained from contour maps can be used in designing new inhibitors.

Conclusions

In this study, molecular docking and 3D-QSAR studies were carried out not only to explore the interaction mechanism between a series of fluoropyrrolidine amides and DP-IV, but also to construct highly accurate and predictive 3D-QSAR models for designing new DP-IV inhibitors for the treatment of diabetes. The modeling results provided a satisfactory explanation for the binding mechanism of fluoropyrrolidine amides with DP-IV. On the basis of the binding conformations of fluoropyrrolidine amide compounds, we have developed stable and predictive 3D-QSAR models with acceptable q^2 values using CoMFA and CoMSIA techniques, and these models could be mapped back to the 3D topology of the binding site of DP-IV. The reliability of the model was verified with compounds in the testing set. The results obtained in this study could provide a powerful tool for predicting the affinity of related compounds with DP-IV, and useful information for guiding further design and synthesis of novel DP-IV inhibitors.

Acknowledgements This work was supported by the National Natural Science Foundation of China (Grants 30600785 and 20572023), the Shanghai Key Basic Research Project (Grant 05JC14092), and the Foundation of East China University of Science and Technology for Research (Grant YC0142101).

References

1. Zimmet P, Alberti KG, Shaw J (2001) Nature 414:782–787
2. Mokdad AH, Ford ES, Bowman BA, Dietz WH, Vinicor F, Bales VS, Marks JS (2003) JAMA 289:76–79
3. Misumi Y, Hyashi Y, Arakawam F, Ikehara Y (1992) Biochim Biophys Acta 1131:333–336
4. Yaron A, Naider F (1993) Crit Rev Biochem Mol Biol 28:31–81
5. Mentlein R (1999) Regul Pept 85:9–24
6. Bell GI, Sanchez-Pescador R, Laybourn PJ, Najarian RC (1983) Nature 304:368–371
7. Majsov S, Henrich G, Wilson IB, Ravazzola M, Orci L, Habner JF (1986) J Biol Chem 261:11880–11889
8. MacInstosh CG, Horowitz M, Verhagen MA, Smout AJ, Wishart J, Morris H, Goble E, Moreley JE, Chapman IM (2001) Am J Gastroenterol 96:997–1007
9. Brubaker PL, Anini Y (2003) J Physiol Pharmacol 81:1005–1012
10. Holst JJ, Deacon DF (1998) Diabetes 47:1663–1670
11. Marguet D, Baggio L, Kobayashi T, Bernard AM, Pierrers M, Nielsen PF, Ribel U, Watanabe T, Drucker DJ, Wagtmann N (2000) Proc Natl Acad Sci USA 97:6874–6879
12. Hughes TE, Mone M D, Russell M E, Weldon S C, Villhauer EB (1999) Biochemistry 38:11597–11603
13. Villhauer EB, Brinkman JA, Naderi GB, Dunning BE, Mangold BL, Mone MD, Russel ME, Welden SC, Hughes TE (2002) J Med Chem 45:2362–2365
14. Villhauer EB, Brinkman JA, Naderi GB, Burkey BF, Dunning BE, Prasad K, Mangold BL, Russell ME, Hughes TE (2003) J Med Chem 46:2774–2789
15. Rasmussen HB, Branner S, Wiberg FC, Wagtmann N (2003) Nature Struct Biol 10:19–25
16. Thoma R, LÖffler B, Stihle M, Huber W, Ruf A, Hennig M (2003) Structure 11:947–959
17. Jens-Uwe P, Weber S, Kritter S, Weiss P, Wallier A, Boehringer M, Hennig M, Kuhn B, Bernd-Michael L (2004) Bioorg Med Chem Lett 14:1491–1493
18. Kim D, Wang LP, Beconi M, Eiermann GJ, Fisher MH, He H, Hickey GJ, Kowalchick JE, Leiting B, Lyons K, Marsilio F, McCann ME, Patel RA, Petrov A, Scapin G, Pates SB, Roy RS, Wu RA, Wyvrtt MJ, Zhang BB, Zhu L, Thornberry NA, Weber AE (2005) J Med Chem 48:141–151
19. Engel M, Hoffmann T, Manhart S, Heiser U, Chambre S, Huber R, Hans-Ulrich D, Bode W (2006) J Mol Biol 355:768–783
20. Nordhoff S, Cerezo-Gálvez S, Feurer A, Hill O, Matassa VG, Metz G, Rummey C, Thiemann M, Edwards PJ (2006) Bioorg Med Chem Lett 16:1744–1748
21. Caldwell CG, Chen P, He JF, Parmee ER, Leiting B, Marsilio F, Patel RA, Wu JK, Eiermann GJ, Petrov A, He H, Lyons KA, Thornberry NA, Weber AE (2004) Bioorg Med Chem Lett 14:1265–1268
22. Brandt W, Lehmann T, Barth A, Fittkaui S (1993) J Mol Graphics 11:277–278
23. Sybyl Version 7.0 (2004) St. Louis (MO), Tripos Associates Inc
24. Clark M, Cramer RDI, Opdenbosch NV (1989) J Comput Chem 10:982–1012
25. Gasteiger J, Marsili M (1980) Tetrahedron 36:3219–3228
26. Weiner SJ, Kollman PA, Case DA, Singh C, Ghio G, Alagona S, Profeta P, Weiner P (1984) J Am Chem Soc 106:765–784
27. Jones G, Willett P, Glen RC, Leach AR, Taylor R (1997) J Mol Biol 267:727–748
28. Eldridge MD, Murray CW, Auton TR, Paolini GV, Mee RP (1997) J Comput Aided Mol Des 11:425–445
29. Cramer RD, Patterson IIIDE, Bunce JD (1988) J Am Chem Soc 110:5959–5967
30. Klebe G, Abraham U, Mietzner T (1994) J Med Chem 37:4130–4146
31. Bohm M, Stuzerbercher J, Klebe G (1999) J Med Chem 42:458–477
32. Edmondson SD, Mastracchio A, Mathvink RJ, He JF, Harper B, Park YJ, Beconi M (2006) J Med Chem 49:3614–3627